Removal of pseudo-convergence in near-coplanar Riemann problems of ideal magnetohydrodynamics and parallel fluid simulations on shared memory processors

Andrew Kercher

George Mason University

28 August 2014

Outline

Introduction
- Shocks in space plasma
- Overview

Riemann problems of ideal MHD

Compound wave formation in ideal MHD

Removing compound wave formation in ideal MHD

Convergence results using new modifcation

Shared memory parallelism

Shocks in space plasma

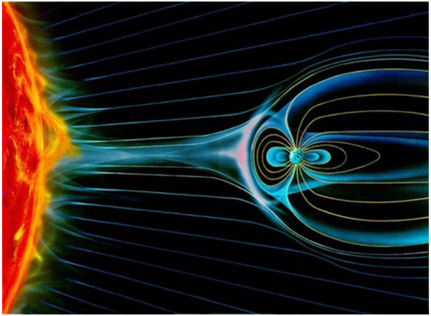

Source [7]

- Sun-earth interaction:
  - Super-sonic plasma originating at sun travels toward earth.

Shocks in space plasma

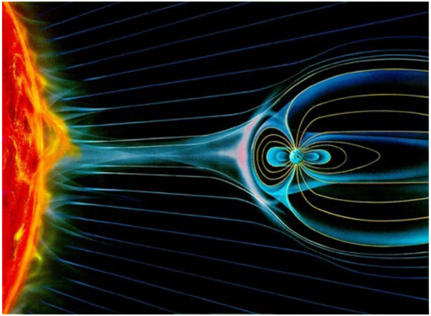

Source [7]

- Sun-earth interaction:
  - Super-sonic plasma originating at sun travels toward earth.
  - Slowed down by magnetic field of Earth.

Shocks in space plasma

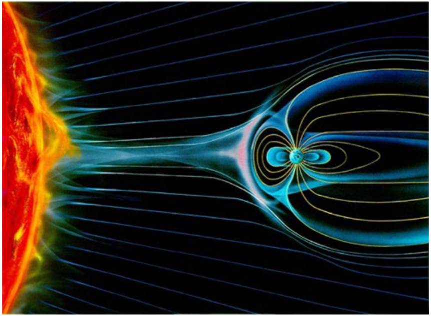

Source [7]

- Sun-earth interaction:
  - Super-sonic plasma originating at sun travels toward earth.
  - Slowed down by magnetic field of Earth.
  - Plasma flow becomes subsonic forming a bow shock.

Shocks in space plasma

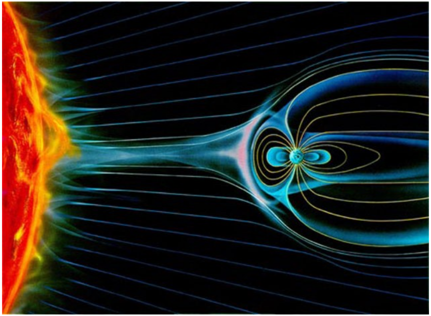

Source [7]

- 2D ideal MHD bow shock simulation. [1]
  - Results contained intermediate shocks.

Shocks in space plasma

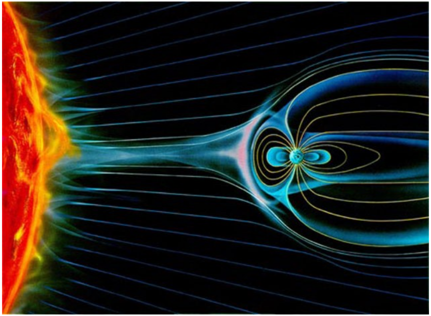

Source [7]

- 2D ideal MHD bow shock simulation. [1]
  - Results contained intermediate shocks.
  - Intermediate shocks considered inadmissible in ideal MHD [4]

Shocks in space plasma

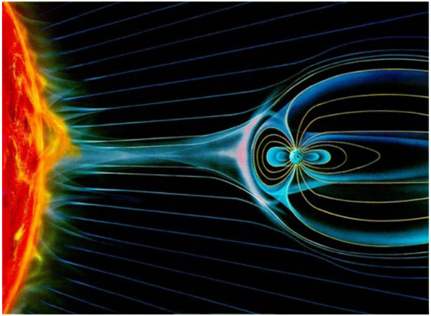

Source [7]

- 2D ideal MHD bow shock simulation. [1]
  - Results contained intermediate shocks.
  - Intermediate shocks considered inadmissible in ideal MHD [4]
  - Cause?

Overview

- Compound wave formation in MHD bow shock simulations.

Overview

- Compound wave formation in MHD bow shock simulations.
- Compound wave product of numerical diffusion.

Overview

- Compound wave formation in MHD bow shock simulations.
- Compound wave product of numerical diffusion.
- Slow convergence with finite volume schemes.

Overview

- Compound wave formation in MHD bow shock simulations.
- Compound wave product of numerical diffusion.
- Slow convergence with finite volume schemes.
- Compound wave modification (CWM).
  - Modification to the HLLD approximate Riemann solver of Athena [8].
  - Removes compound wave, correctly computes rotational discontinuity.
  - Converges at all grid resolutions.
  - FAST! HLLD intermediate states are already calculated.

Overview

- Compound wave formation in MHD bow shock simulations.
- Compound wave product of numerical diffusion.
- Slow convergence with finite volume schemes.
- Compound wave modification (CWM).
  - Modification to the HLLD approximate Riemann solver of Athena [8].
  - Removes compound wave, correctly computes rotational discontinuity.
  - Converges at all grid resolutions.
  - FAST! HLLD intermediate states are already calculated.
- Description multi-dimensional fluid solver capable of shared memory parallelism.
  - Hydrodynamics and ideal MHD.
  - Algorithms implemented for unstructured grids.

Outline

Ideal magnetohydrodynamics

$$
\begin{aligned}
\frac{\partial \rho}{\partial t} + \nabla \cdot (\rho \mathbf{v}) = 0 \ , \\
\frac{\partial (\rho \mathbf{v})}{\partial t} + \nabla \cdot \left[\rho \mathbf{v} \otimes \mathbf{v} + \left(p_g + \frac{B^2}{2} \right) \underline{\mathbf{I}} - \mathbf{B} \otimes \mathbf{B} \right] = 0 \ , \\
\frac{\partial E}{\partial t} + \nabla \cdot \left[\left(E + p_g + \frac{B^2}{2} \right) \mathbf{v} - \mathbf{v} \cdot \mathbf{B} \otimes \mathbf{B} \right] = 0 \ , \text{ and} \\
\frac{\partial \mathbf{B}}{\partial t} + \nabla \cdot [\mathbf{v} \otimes \mathbf{B} - \mathbf{B} \otimes \mathbf{v}] = 0 \ ,
\end{aligned}
$$

where the energy density is defined as

$$
E = \frac{p_g}{\gamma - 1} + \frac{\rho v^2}{2} + \frac{B^2}{2} \ ,
$$

Ideal magnetohydrodynamics

Non-strictly hyperbolic.

$$\frac{\partial \mathbf{U}}{\partial t} + \frac{\partial \mathbf{F}}{\partial x} = 0.$$

Real, but **not** necessarily distinct eigenvalues:

$$\begin{aligned} v_n &: \text{contact or tangential discontinuity (entropy)}, \\ v_n \pm c_s &: \text{slow rarefaction or shock}, \\ v_n \pm c_a &: \text{rotational discontinuity (Alfvén), and} \\ v_n \pm c_f &: \text{fast rarefaction or shock}, \end{aligned}$$

$$c_{f,s}^2 = \frac{1}{2}\left[a^2 + c_a^2 + c_t^2 \pm \sqrt{\left(a^2 + c_a^2 + c_t^2\right)^2 - 4a^2 c_a^2}\right],$$

$$c_a^2 = \frac{B_n^2}{\rho}, \text{ and } c_t^2 = \frac{B_t^2}{\rho}.$$

HLLD approximate Riemann solver

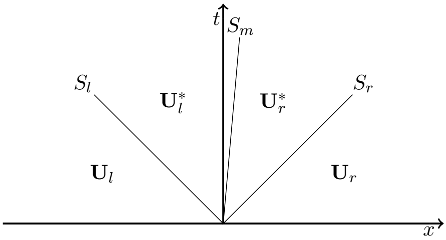

- HLLD [5] (D for *discontinuities*) extention of HLLC to MHD.

HLLD approximate Riemann solver

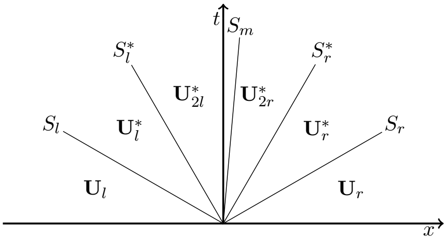

- HLLD [5] (D for *discontinuities*) extention of HLLC to MHD.
- Restores rotational discontinuity.

Riemann problems of ideal MHD

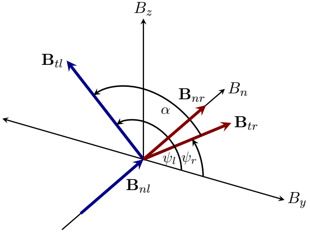

- Initial discontinuity separates two states.
- Rotation angle: $\psi = \arctan\left(B_z/B_y\right)$.
- Twist angle: $\alpha = \psi_r - \psi_l$.

Riemann problems of ideal MHD

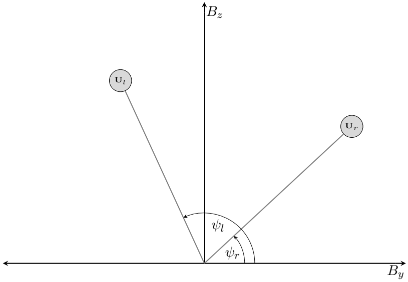

- Regular waves alter magnitude or orientation of B_t.

Riemann problems of ideal MHD

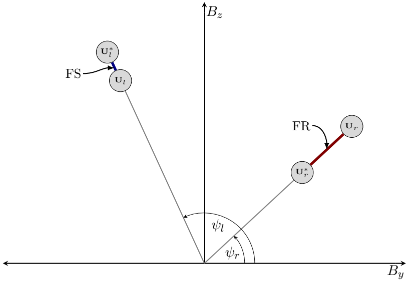

- Regular waves alter magnitude or orientation of B_t.
- Fast shock: $B_t \uparrow$, fast rarefaction: $B_t \downarrow$.

Riemann problems of ideal MHD

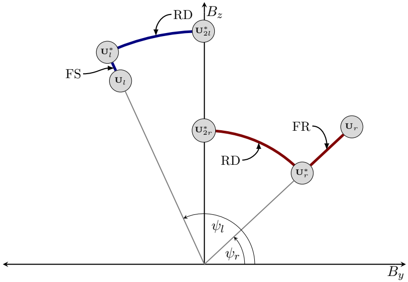

- Regular waves alter magnitude or orientation of B_t.
- Fast shock: $B_t \uparrow$, fast rarefaction: $B_t \downarrow$.
- Rotational discontinuity: $\psi \pm \delta\psi$.

Riemann problems of ideal MHD

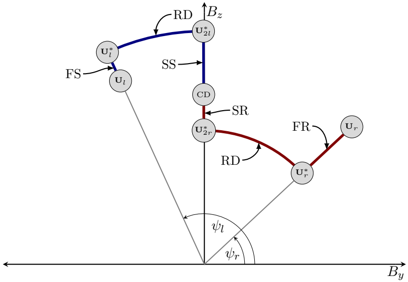

- Regular waves alter magnitude or orientation of B_t.
- Fast shock: $B_t \uparrow$, fast rarefaction: $B_t \downarrow$.
- Rotational discontinuity: $\psi \pm \delta\psi$.
- Slow shock: $B_t \downarrow$, slow rarefaction: $B_t \uparrow$.

Riemann problems of ideal MHD

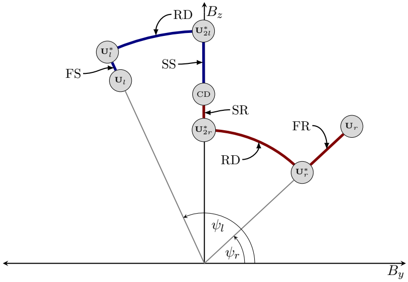

- Regular waves alter magnitude or orientation of B_t.
- Fast shock: $B_t \uparrow$, fast rarefaction: $B_t \downarrow$.
- Rotational discontinuity: $\psi \pm \delta\psi$.
- Slow shock: $B_t \downarrow$, slow rarefaction: $B_t \uparrow$.
- Contact discontinuity: no change.

Riemann problems of ideal MHD

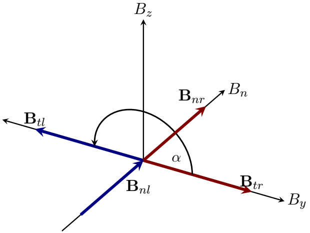

- Coplanar magnetic field

Outline

Non-unique solutions

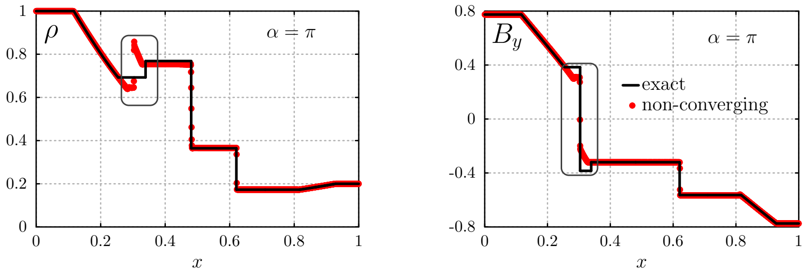

- Solutions to coplanar Riemann problems of ideal MHD are non-unique.
- At $x = 0.303$, rotational discontinuity $\rightarrow$ compound wave.

Non-unique solutions

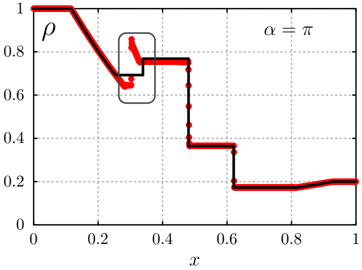

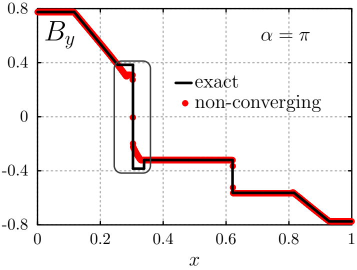

- Solutions to coplanar Riemann problems of ideal MHD are non-unique.
- At $x = 0.303$, rotational discontinuity $\rightarrow$ compound wave.
- Compound wave is composed of an intermediate shock and a slow rarefaction.
- Physical?

Non-unique solutions

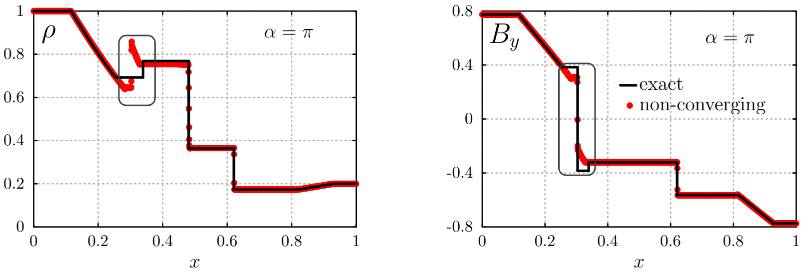

- Solutions to coplanar Riemann problems of ideal MHD are non-unique.
- At $x = 0.303$, rotational discontinuity $\rightarrow$ compound wave.
- Compound wave is composed of an intermediate shock and a slow rarefaction.
- Physical?
  - Unstable for under small perturbations [4].

Non-unique solutions

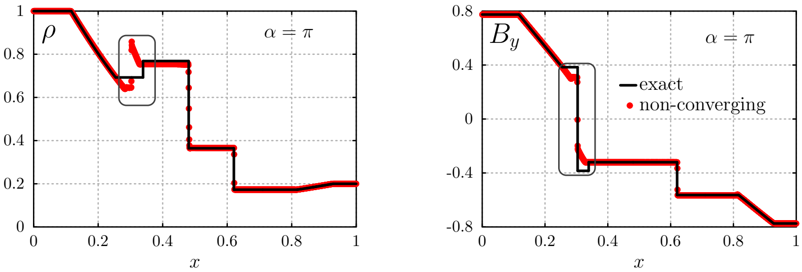

- Solutions to coplanar Riemann problems of ideal MHD are non-unique.
- At $x = 0.303$, rotational discontinuity $\rightarrow$ compound wave.
- Compound wave is composed of an intermediate shock and a slow rarefaction.
- Physical?
  - Unstable for under small perturbations [4].
  - Satisfy jump conditions (coplanar case).

Compound wave formation

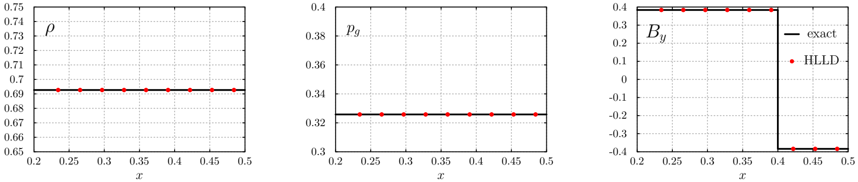

- Compound waves are a product of numerical diffusion.

Compound wave formation

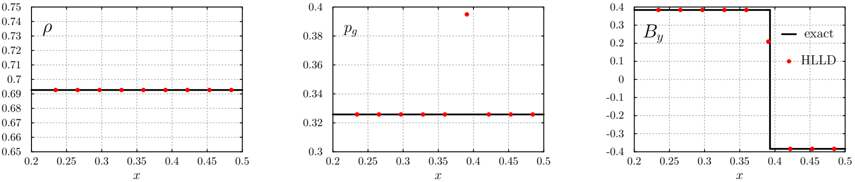

- Compound waves are a product of numerical diffusion.
- Decrease $B_t \rightarrow$ increase p_g

$$p_g = (\gamma - 1)\left(E - \frac{\rho v^2}{2} - \frac{B^2}{2}\right)$$

Compound wave formation

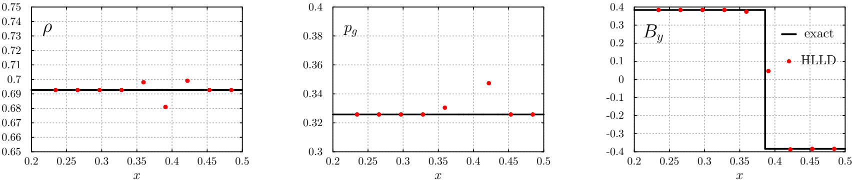

- Compound waves are a product of numerical diffusion.
- Decrease $B_t \rightarrow$ increase p_g

$$p_g = (\gamma - 1)\left(E - \frac{\rho v^2}{2} - \frac{B^2}{2}\right)$$

- Increase $p_g \rightarrow$ compound wave.

Psuedo-convergence

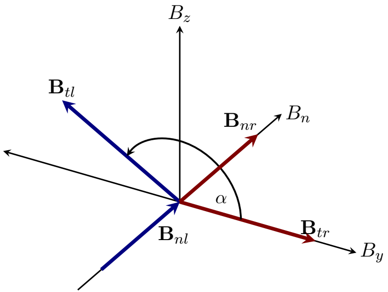

- $\alpha < \pi$, compound waves at lower resolutions.

Psuedo-convergence

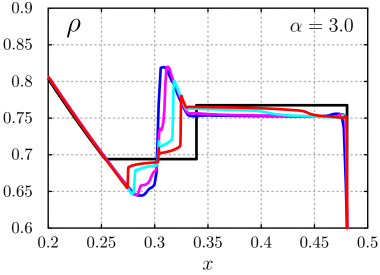

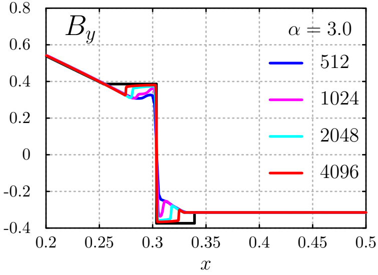

- $\alpha < \pi$, compound waves at lower resolutions.
- Psuedo-convergence: rotational discontinuity at higher resolutions [9].
- Transition between 1024 and 2048 grid points.
- $\alpha \to \pi$, grid resolution increases.
- $\pi = \alpha$, compound wave at all resolutions.

Outline

Compound wave modification

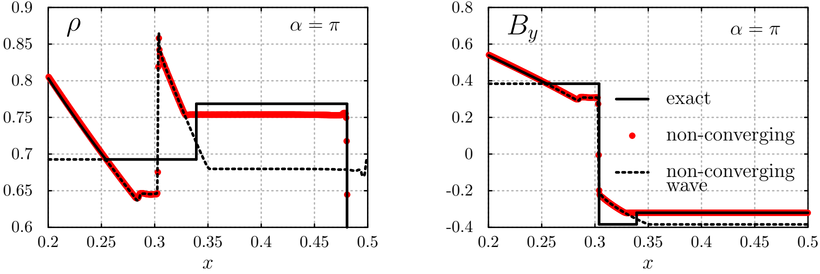

- Need to reduce numerical diffusion.

Compound wave modification

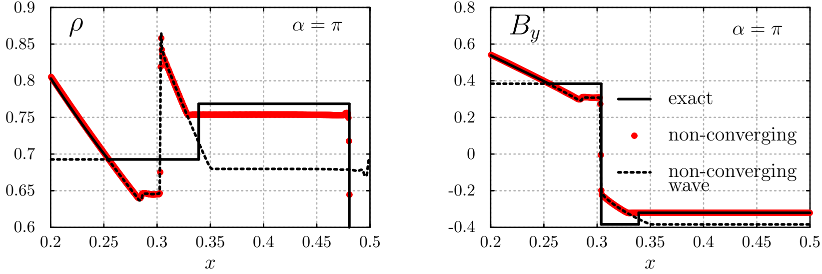

- Need to reduce numerical diffusion.
- ρ and B_t should remain constant across the rotational discontinuity $x = 0.303$.

Compound wave modification

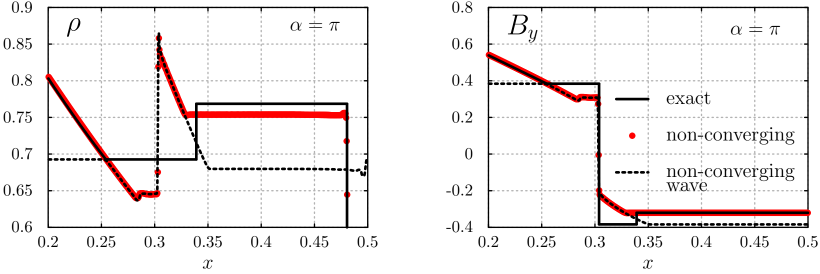

- Need to reduce numerical diffusion.
- ρ and B_t should remain constant across the rotational discontinuity $x = 0.303$.
- Limit flux associated with the compound wave.

Compound Wave modification

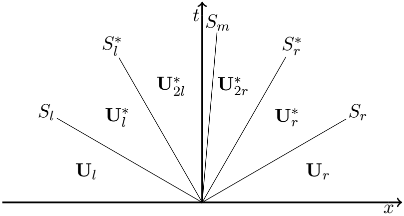

- Use HLLD to approximate intermediate states upstream and downstream of rotational discontinuity, i.e., $\mathbf{U}_\mathbf{l}^*$ and $\mathbf{U}_{2l}^*$.

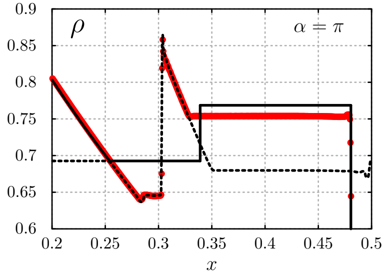

Compound Wave modification

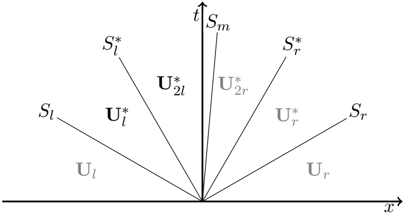

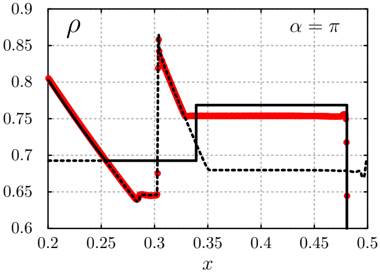

- Use HLLD to approximate intermediate states upstream and downstream of rotational discontinuity, i.e., $\mathbf{U}_\mathbf{l}^*$ and $\mathbf{U}_{2l}^*$.
- Calculate flux $\mathbf{F}^c$ between $\mathbf{U}_\mathbf{l}^*$ and $\mathbf{U}_{2l}^*$.

Compound Wave modification

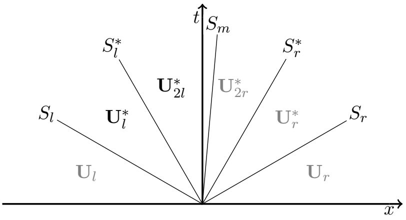

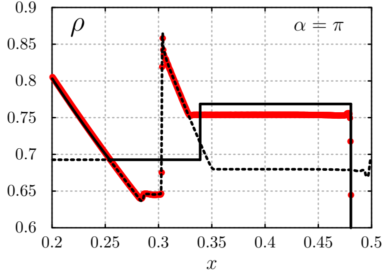

- Use HLLD to approximate intermediate states upstream and downstream of rotational discontinuity, i.e., $\mathbf{U}_\mathbf{l}^*$ and $\mathbf{U}_{2l}^*$.
- Calculate flux $\mathbf{F}^c$ between $\mathbf{U}_\mathbf{l}^*$ and $\mathbf{U}_{2l}^*$.
- Reduce the contribution of $\mathbf{F}^c = \mathbf{F}_{hlld}(\mathbf{U}_l^*, \mathbf{U}_{l2}^*)$ to the total flux.

Compound Wave modification

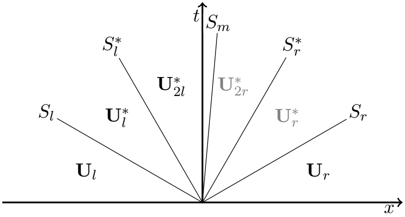

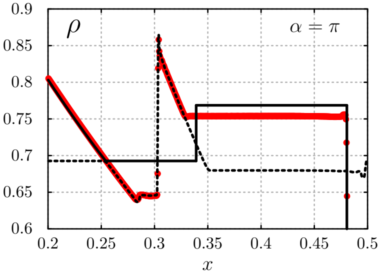

- Use HLLD to approximate intermediate states upstream and downstream of rotational discontinuity, i.e., $\mathbf{U}_\mathbf{l}^*$ and $\mathbf{U}_{2l}^*$.
- Calculate flux $\mathbf{F}^c$ between $\mathbf{U}_\mathbf{l}^*$ and $\mathbf{U}_{2l}^*$.
- Reduce the contribution of $\mathbf{F}^c = \mathbf{F}_{hlld}(\mathbf{U}_l^*, \mathbf{U}_{l2}^*)$ to the total flux.
- $\mathbf{F}_{cwm} = \mathbf{F}_{hlld}(\mathbf{U}_l, \mathbf{U}_r) - A\mathbf{F}^c$, where $A < 0.5$.

CWM solution

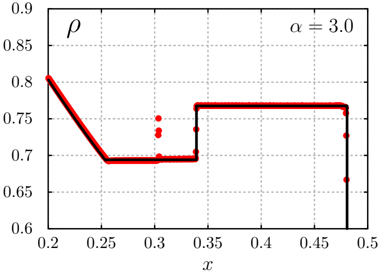

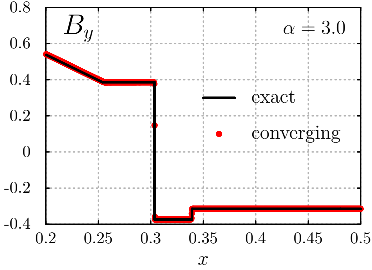

- CWM recovers the correct solution upstream and downstream of rotational discontinuity.
- Transition across rotational discontinuity is unresolved.
- Resolve it?

CWM solution

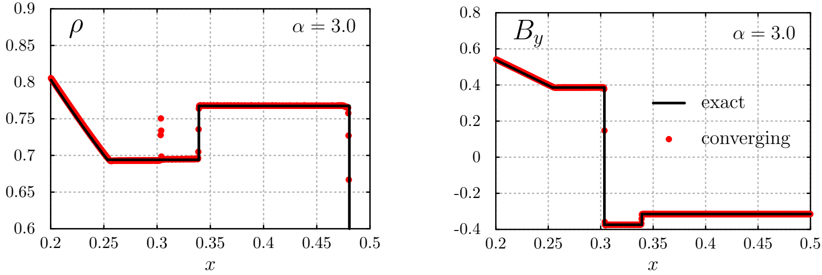

- CWM recovers the correct solution upstream and downstream of rotational discontinuity.
- Transition across rotational discontinuity is unresolved.
- Resolve it?
- Simple but non-conservative.

CWM Resolving the transition

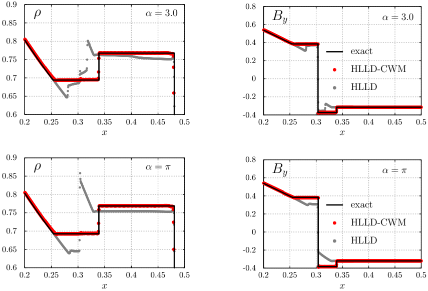

- Jump conditions in Lagrangian mass coordinates, $V = 1/\rho$, W is wave speed.
- Brackets denote difference across discontinuity.

$$W[V] = -[v_n],$$
$$W[v_n] = -[P - B_n^2],$$
$$W[\mathbf{v}_t] = -B_n[\mathbf{B}_t],$$
$$W[V\mathbf{B}_t] = -B_n[\mathbf{v}_t],$$

CWM Resolving the transition

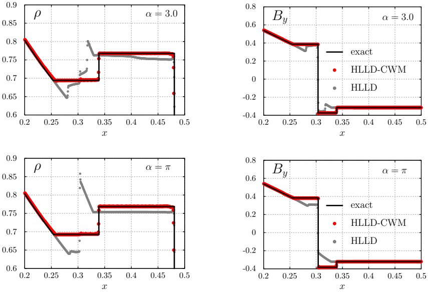

- Across rotational discontinuity

$$
\begin{aligned}
[V] &= 0, \\
[v_n] &= 0, \\
[p_g] &= 0, \\
[B_t] &= 0, \\
W[\mathbf{v}_t] &= -B_n[\mathbf{B}_t],
\end{aligned}
$$

- $W = \sqrt{\rho} B_n$ is Lagrangian speed of linear wave.

Examples

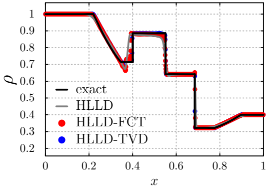

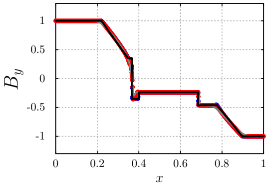

- Near coplanar initial conditions.
- Fast compound wave at $x = 0.365$

Examples

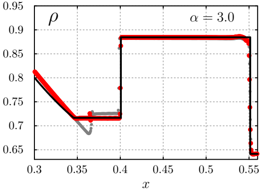

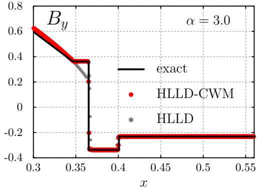

- Near coplanar initial conditions.
- Fast compound wave at $x = 0.365$
- Small deviation for weak intermediate shocks.

Examples

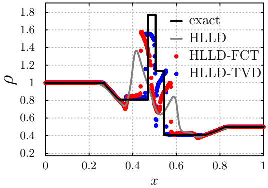

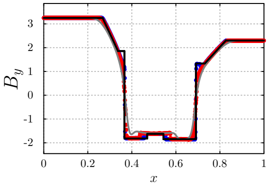

- Non-planar initial conditions.
- Fast compound waves at $x = 0.366$ and $x = 0.691$

Examples

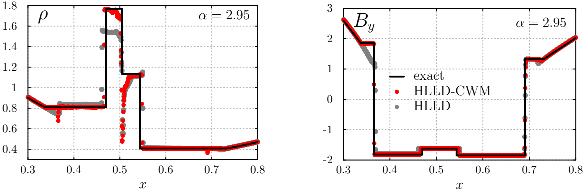

- Non-planar initial conditions.
- Fast compound waves at $x = 0.366$ and $x = 0.691$
- Small deviation for weak intermediate shocks.

Outline

Introduction

- Shocks in space plasma
- Overview

Riemann problems of ideal MHD

Compound wave formation in ideal MHD

Removing compound wave formation in ideal MHD

Convergence results using new modifcation

Shared memory parallelism

Error analysis

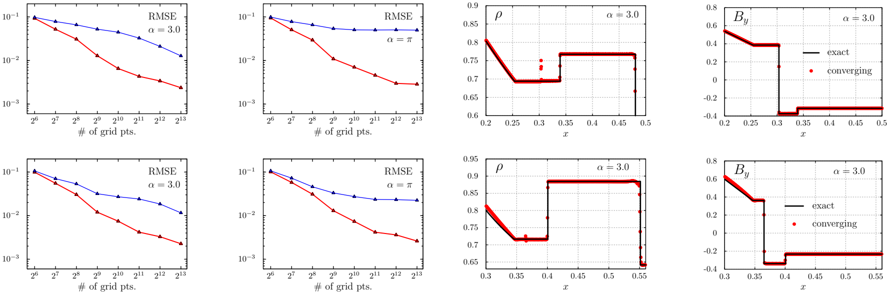

- Error calculation without applying the correction at the rotational discontinuity.
- Without CWM, the compoiund wave starts to break apart between 2^{10} and 2^{11}.
- CWM produces convergence at low grid resolutions.

Outline

Higher dimensions

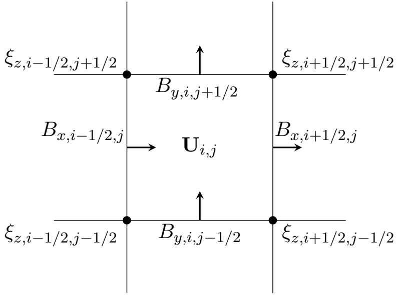

Maintaining $\nabla \cdot \mathbf{B} = 0$ with constrained transport [2].

- Staggered grid.
- Hydrodynamical variables at cell centers.
- Magnetic field at interface.
- $\mathbf{E} = -\mathbf{v} \times \mathbf{B}$ at corners.
- Denote z-component of the emf as ξ_z.

Finite area integration of interface **B**

$$B^{n+1}_{x,i+1/2,j} = B^{n}_{x,i+1/2,j} - \frac{\delta t}{\delta y}\left(\xi_{z,i+1/2,j+1/2} - \xi_{z,i+1/2,j-1/2}\right)$$

$$B^{n+1}_{y,i,j+1/2} = B^{n}_{y,i,j+1/2} + \frac{\delta t}{\delta x}\left(\xi_{z,i+1/2,j+1/2} - \xi_{z,i-1/2,j-1/2}\right)$$

Higher dimensions

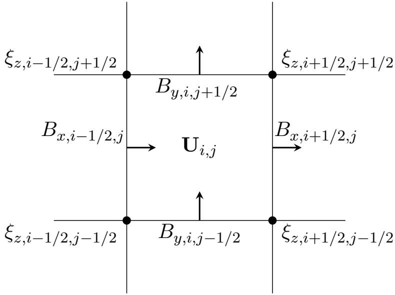

Maintaining $\nabla \cdot \mathbf{B} = 0$ with constrained transport [2].

- Staggered grid.
- Hydrodynamical variables at cell centers.
- Magnetic field at interface.
- $\mathbf{E} = -\mathbf{v} \times \mathbf{B}$ at corners.
- Denote z-component of the emf as ξ_z.

Due to perfect cancellation, the numerical divergence in the cell remains zero to machine precision.

$$(\nabla \cdot \mathbf{B})_{i,j} = \frac{1}{\delta x}\left(B_{x,i+1/2,j} - B_{x,i-1/2,j}\right) + \frac{1}{\delta y}\left(B_{y,i,j+1/2} - B_{y,i,j-1/2}\right)$$

Shared memory parallelism

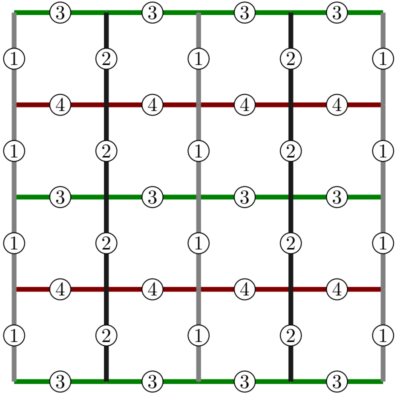

- Faces must be grouped by color to avoid memory contention.
- Loop over the faces becomes loop over the colors.

Shared memory parallelism

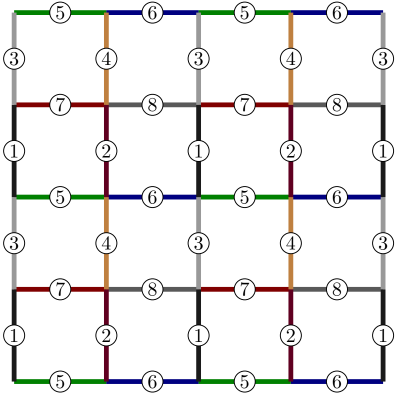

- Faces must be grouped by color to avoid memory contention.
- Loop over the faces becomes loop over the colors.
- Constrained transport, faces and edges must be colored.

Efficient algorithms

```
thrust::device_vector<float> x(n);  // independent
    variable
thrust::device_vector<float> y(n);  // y = f(x)
thrust::device_vector<float> z(n);  // z = g(y)

// compute y = f(x)
thrust::transform(x.begin(),x.end(),y.begin(),f());

// compute z = g(y)
thrust::transform(y.begin(),y.end(),z.begin(),g());
```

- Function composition [3].
- $3n$ floats, $2n$ reads, $2n$ writes, and uses n temporary floats.

Efficient algorithms

```
thrust::device_vector<float> x(n);  // independent
    variable
thrust::device_vector<float> z(n);  // z = g(y) = g(
    f(x))

// compute z = g(f(x))
thrust::transform(make_transform_iterator(x.begin(),
    f()),
                  make_transform_iterator(x.end(),f
                      ()),
                  z.begin(),
                  g());
```

- Function composition [3].
- $2n$ floats, n reads, n writes, and no temporary storage.

Memory access

```
struc
    conservative_variables{
  float density;
  float momentum_x;
  float energy;
}

conservative_variables
  *state;  // AoS

state[i].density =
    some_number;
state[i].momentum_x =
    another_number;
state[i].energy =
    one_more_number;
```

```
struc
    conservative_variables{
  float *density;
  float *momentum_x;
  float *energy;
}

conservative_variables
    state; // SoA

state.density[i] =
    some_number;
state.momentum_x[i] =
    another_number;
state.energy[i] =
    one_more_number;
```

- Memory coalescing occurs when multiple memory addresses are accessed with a single transaction.
- Memory does not coalesce with AoS (left).
- Memory does coalesce with SoA (right).

Memory access

```
thrust::device_vector<primitive_variables>
     primitive_state(n);  // AoS
thrust::device_vector<conservative_variables>
     conservative_state(n);   // AoS
thrust::transform_n(primitive_state.begin(),
                    primitive_state.size(),
                    conservative_state.begin(),
                    convert_primitive_to_conservative(
                        gamma));
```

- Converting from primitive variables (ρ, v_x, p_g) to conservative variables $(\rho, \rho v_x, en)$.
- No coalescing.

Memory access

```
thrust::device_vector<float> d(n),vx(n),pg(n);
thrust::device_vector<float> mx(n),en(n);
thrust::transform_n(
          thrust::make_zip_operator(
            make_tuple(d.begin(),
                       vx.begin(),
                       pg.begin())),
           n,
           thrust::make_zip_operator(
             make_tuple(d.begin(),
                        mx.begin(),
                        en.begin())),
           convert_primitive_to_conservative(gamma));
```

- Converting from primitive variables (ρ, v_x, p_g) to conservative variables $(\rho, \rho v_x, en)$.
- Arrays can be combined on the fly with a `zip_operator` to achieve coalescing.

Performance Comparison

Performance comparison for Orszag-Tang [6] test.

grid size	cells/second (GPU)	cells/second (CPU)	ratio
64×64	4.1894×10^6	7.3955×10^5	5
128×128	1.6540×10^7	7.5060×10^5	22
256×256	4.4497×10^7	7.3155×10^5	60
512×512	6.3286×10^7	7.9437×10^5	79
1024×1024	7.2134×10^7	8.3354×10^5	86

- Dell Precision 7500 workstation with a (Dual CPU)
- CPU Intel Xeon E5645 @ 2.40 Ghz.
- GPU GeFroce GTX TITAN with a memory bandwidth of 288.4 GB/sec and 2688 CUDA cores.
- Almost a factor of three increase of speed ratio form 128×128 to 256×256.

Conclusion

- Compound wave modification:
  - Produces rotational discontinuity for coplanar problems.
  - Removes pseudo-convergence for near coplanar problems.
  - Does not require exact solver.
  - FAST! HLLD intermediate states are already calculated.
  - Produces the correct result when other numerical inaccuracies are present.
- Parallel fluid solver.
  - General geometry on unstructured grids.
  - Capable of shared memory parallelism on GPU and CPU.

Bibliography I

[1] H. de Sterck, B. C. Low, and S. Poedts. "Complex magnetohydrodynamic bow shock topology in field-aligned low-β flow around a perfectly conducting cylinder". In: *Physics of Plasmas* 5 (Nov. 1998), pp. 4015–4027.

[2] C. R. Evans and J. F. Hawley. "Simulation of magnetohydrodynamic flows - A constrained transport method". In: *ApJ* 332 (Sept. 1988), pp. 659–677.

[3] Jared Hoberock and Nathan Bell. *Thrust: A Parallel Template Library*. Version 1.7.0. 2010. URL: http://thrust.github.io/.

[4] L. D. Landau, E. M. Lifshitz, and L. P. Pitaevskii. *Electrodynamics of continuous media*. 3rd. 1984.

Bibliography II

[5] T. Miyoshi and K. Kusano. "A multi-state HLL approximate Riemann solver for ideal MHD". In: *J. Comp. Phys.* 208 (May 2005), pp. 315–344.

[6] S. A. Orszag and C.-M. Tang. "Small-scale structure of two-dimensional magnetohydrodynamic turbulence". In: *Journal of Fluid Mechanics* 90 (Jan. 1979), pp. 129–143.

[7] *Spasce Weather*. `http://now.uiowa.edu/files/now.uiowa.edu/styles/prim_horizontal_640/public/sun-earth-640.jpg?itok=ESKVX0GJ`.

[8] J. Stone, T. Gardner, and P. Teuben. *Athena MHD Code Project*. `https://trac.princeton.edu/Athena/`. Dec. 2010.

Bibliography III

[9] M. Torrilhon. “Non-uniform convergence of finite volume schemes for Riemann problems of ideal magnetohydrodynamics”. In: *J. Comp. Phys.* 192 (Nov. 2003), pp. 73–94.